Biochemistry

pubs.acs.org/biochemistry Article

Caspase-9 Activation of Procaspase-3 but Not Procaspase-6 Is Based on the Local Context of Cleavage Site Motifs and on Sequence

Ishankumar V. Soni and Jeanne A. Hardy*

Cite This: *Biochemistry* 2021, 60, 2824−2835 Read Online

ABSTRACT: Studying the interactions between a protease and its protein substrates at a molecular level is crucial for identifying the factors facilitating selection of particular proteolytic substrates and not others. These selection criteria include both the sequence and the local context of the substrate cleavage site where the active site of the protease initially binds and then performs proteolytic cleavage. Caspase-9, an initiator of the intrinsic apoptotic pathway, mediates activation of executioner procaspase-3 by cleavage of the intersubunit linker (ISL) at site ^{172}IETD↓S. Although procaspase-6, another executioner, possesses two ISL cleavage sites (site 1, ^{176}DVVD↓N; site 2, ^{190}TEVD↓A), neither is directly cut by caspase-9. Thus, caspase-9 directly activates procaspase-3 but not procaspase-6. To elucidate this selectivity of caspase-9, we engineered constructs of procaspase-3 (e.g., swapping the ISL site, ^{172}IETD↓S, with DVVDN and TEVDA) and procaspase-6 (e.g., swapping site 1, ^{176}DVVD↓N, and site 2, ^{190}TEVD↓A, with IETDS). Using the substrate digestion data of these constructs, we show here that the P4−P1′ sequence of procaspase-6 ISL site 1 (DVVDN) can be accessed but not cleaved by caspase-9. We also found that caspase-9 can recognize the P4−P1′ sequence of procaspase-6 ISL site 2 (TEVDA); however, the local context of this cleavage site is the critical factor that prevents proteolytic cleavage. Overall, our data have demonstrated that both the sequence and the local context of the ISL cleavage sites play a vital role in preventing the activation of procaspase-6 directly by caspase-9.

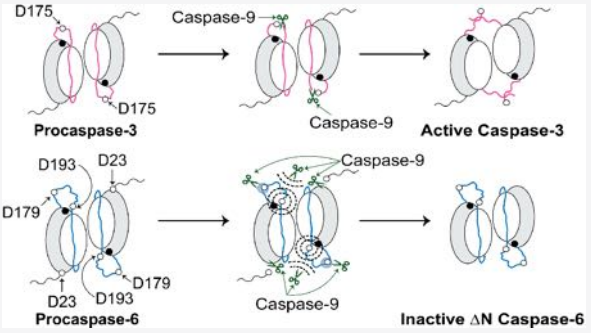

Proteolysis, a process of enzymes catalyzing the hydrolytic cleavage of their substrates, drives various biological pathways (e.g., cell cycle,[1] cell differentiation,[2] and cell death[3]) to maintain homeostasis in all living organisms. Examining the interactions between a particular protease and its protein substrate at a molecular level is beneficial in understanding their involvement in particular biological pathways. The Schechter−Berger convention has been widely adopted by the protease community to showcase the interactions between the peptide residues in the substrate cleavage site (denoted as P) and subsites of the protease active site (denoted as S), where the cleavage (↓) occurs between P1 and P1′ (Figure 1A).[4] The nature of the subsites on the enzyme together with the cleavage site motif within the substrate is considered to define protease preference. This notion is reinforced when the broad range of sequences detected by protein or peptide-based protease substrate profiling are reduced to a single "preferential" cleavage motif. In contrast to this narrow view of recognition specificity, detailed analyses of aggregate data on proteolysis suggest that reducing the concept of recognition motif to a single sequence is overly simplistic. For example, the preferred cleavage motif of caspase-7 protease using peptide-based screening[5] or proteomics[6] was identified as DEVD↓ (P4−P1) and DEVD↓G (P4−P1′), respectively. However, from the same proteomics study's data, we found that, of 128 peptides cleaved by caspase-7, the cleavage sites of DEVD↓G, DEVD↓X, and DXXD↓X were only 2, 4, and 36, respectively.[6] Another example is the family of ClpP proteases (from *Escherichia coli*, *Staphylococcus aureus*, and human mitochondria) that favor peptide substrates composed of specific residues at the P3−P1 positions (e.g., natural amino acids preferred by human mitochondria ClpP at P3−P1 positions are F/W-M/T/L-M/L); nonetheless, proteomics studies of these proteases revealed a very weak cleavage preference.[7] In fact, it was later discovered that proteolysis by ClpP protease (from *Caulobacter crescentus*) complexed with ClpX (an unfoldase that feeds ClpP) is mainly governed by local context (substrate cleavage occurred after every 10−13 residues) and not dependent on sequence.[8] Upon examination of the cleavage preferences for any protease and its suite of cleaved substrates, it becomes clear that (i) no single peptide sequence can fully account for the cleavage properties observed for a natural protease and (ii) the sequence specificity alone cannot completely account for the selection of substrates that

Received: July 2, 2021
Revised: August 26, 2021
Published: September 2, 2021

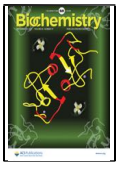

https://doi.org/10.1021/acs.biochem.1c00459
Biochemistry 2021, 60, 2824−2835

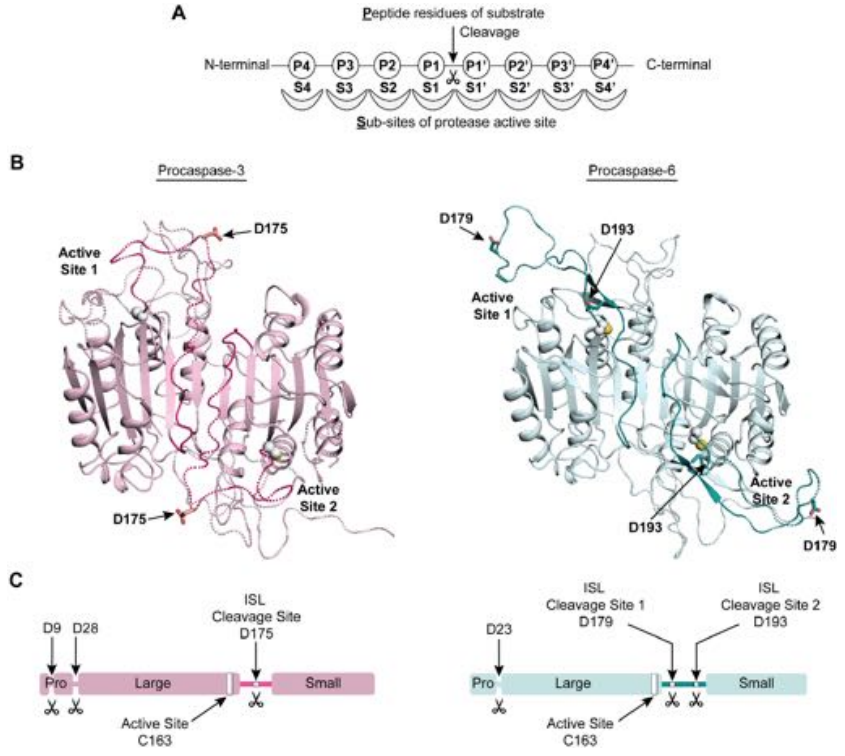

Figure 1. Procaspase-3 and -6 share the same core structural fold, and intersubunit linker (ISL) cleavage is a prerequisite for their activation. (A) Schechter−Berger schematic diagram representing protease specificity toward the cleavage sequence of the substrates.[4] Peptide residues of the substrates and subsites of protease active site are denoted as P and S, respectively. The cleavage of substrate occurs at the amide bond between the residues at positions P1 and P1′. Caspases prefer aspartate at the P1 position. (B) Procaspase-3 (light pink) and procaspase-6 (light cyan) structures with the missing loops and/or regions shown as dashes, which were modeled as described in Materials and Methods. The Protein Data Bank entries used to model procaspase-3 and -6 were 4JQY and 3NR2, respectively. The active site cysteines of both procaspases were substituted with alanine (C163A) to determine the structures of full-length uncleaved zymogen.[25,26] Active site cysteines (substituted for alanine present in the original structures by using the mutagenesis feature of PyMOL) of procaspase-3 and -6 are shown as spheres. Both procaspases possess a similar overall structural fold in the core. The greatest differences are present in the mobile loops. Loops containing the ISL are highlighted (dark pink for procaspase-3 and dark cyan for procaspase-6). Procaspase-3 has a known ISL cleavage after D175 (P1 position),[19,20] and procaspase-6 has two known ISL cleavages after D179 and D193.[21] (C) Linear cartoons of procaspase-3 and -6 illustrating their prodomain (N), large subunit (Lg), ISL, and small subunit (Sm). Simply removing the prodomain from both procaspases is not sufficient for their activation. ISL cleavage is required in both procaspases for activation.[41,42]

are cleaved. Thus, we hypothesized at the outset of this work that both the sequence and the local context of the substrate cleavage site may be important factors governing recognition by a protease.

One prime example of the gulf between canonical recognition sequence and the actual cleavage propensity is exemplified in the caspases. Caspases are cysteine-aspartate proteases that play key roles in regulating multiple cellular pathways, including apoptosis and inflammation. Dysfunction in caspase regulation is a hallmark of several diseases such as cancers,[9,10] autoimmune disorders,[11,12] and neurodegeneration.[13,14] Therefore, it is important to understand their cellular pathways at a molecular level. The defining feature of this family of proteases is their ability to cleave substrates at sites containing aspartate at the P1 position (Figure 1A), although glutamate and phosphoserine can also be recognized, albeit at low frequencies.[15,16] Apoptotic caspases are categorized into two groups: initiators (caspase-8, -9, and -10) and executioners (caspase-3, -6, and -7). Caspases are translated as full-length, inactive zymogens termed procaspases. Initiator zymogens are recruited to activation platforms upon either intrinsic (e.g., procaspase-9 to form the apoptosome)[17] or extrinsic (e.g., procaspase-8 to form the death-inducing signaling complex)[18] cell signaling to dimerize and ultimately achieve maturation. If the mobile loops are excluded, executioner zymogens possess similar structural folds (Figure 1B) and are activated by a cleavage event at their intersubunit linker (ISL) generating large and small subunits (Lg and Sm, respectively) from each chain of the procaspase dimer (Figure 1C). Procaspase-3 has one ISL cleavage site at D175,[19,20] while procaspase-6 has two ISL cleavage sites, D179 and D193[21] (Figure 1B,C). In an intrinsic apoptotic pathway, upon its activation, caspase-9 cleaves the ISL of procaspase-3 and -7, thereby activating them to the mature form. Activated caspase-3 mediates procaspase-6 ISL cleavage to activate caspase-6.[22−24] Activated executioners proteolyze their respective and common substrates evoking apoptosis. In this work, we sought to address a key question in the field: Why can caspase-9 cleave the ISLs of procaspase-3 and -7 but not the procaspase-6 ISL cleavage sites? Addressing this question, while providing insights for caspase-9, can also be applied to proteases and their substrate selection generally.

MATERIALS AND METHODS

Generation of Full-Length Procaspase-3 and -6 Models by Adding Missing Residues. We generated full-length models of procaspase-3 and -6 by employing structures from the Protein Data Bank (PDB): 4JQY and 3NR2, respectively.[25,26] The missing residues of procaspase-3 (1−31,

https://doi.org/10.1021/acs.biochem.1c00459
Biochemistry 2021, 60, 2824−2835

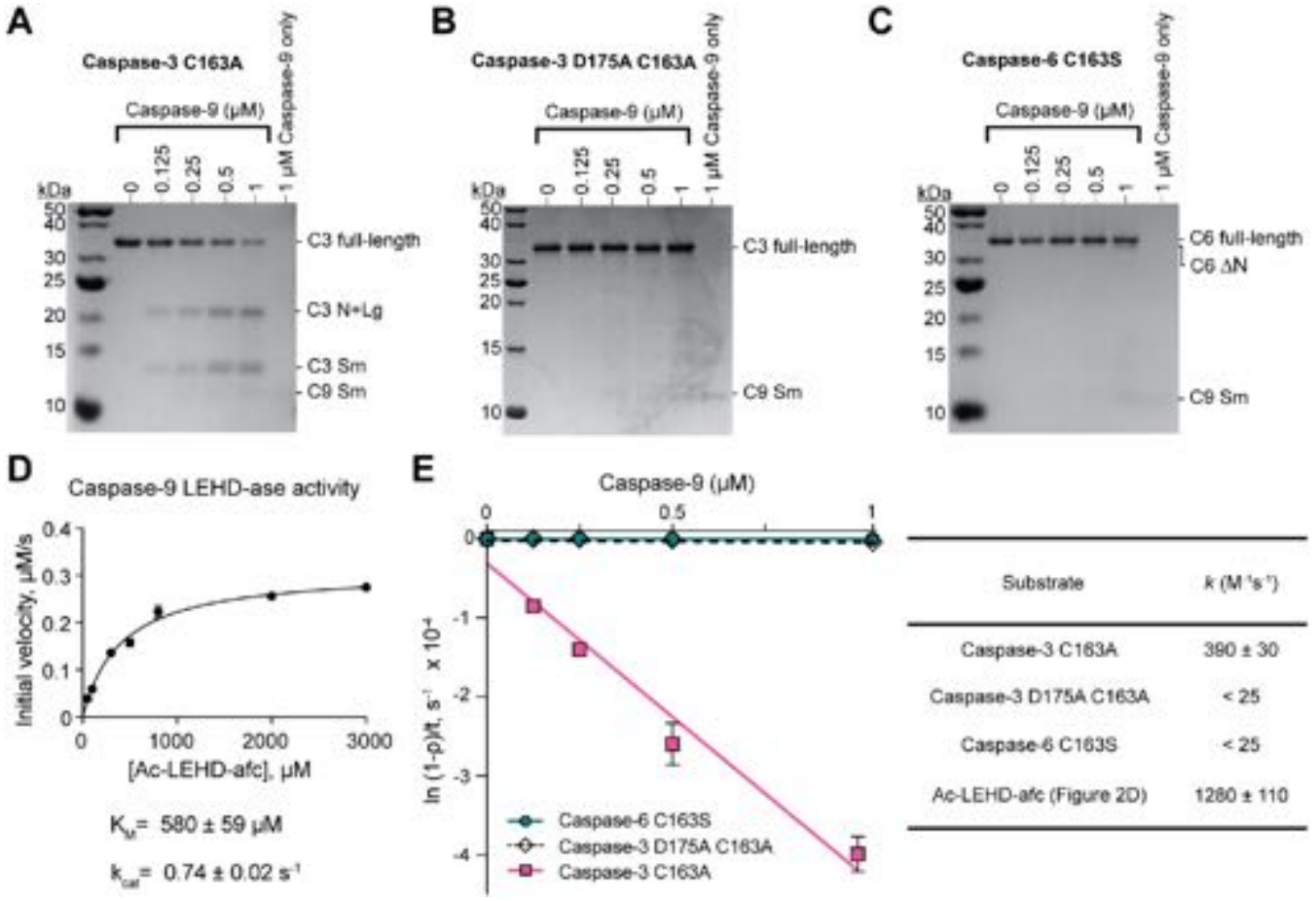

Figure 2. Caspase-9 cleaves the ISL of procaspase-3 but not procaspase-6. (A−C) Different concentrations of recombinant wild-type caspase-9 ranging from 0 to 1 μM were incubated with 3 μM recombinant procaspase-3 (caspase-3 C163A), caspase-3 C163A D175A, and procaspase-6 (caspase-6 C163S), respectively, for 1 h at 37 °C. In the last lane of each gel, 1 μM caspase-9 was added as a control. Caspase-9 cleaved (A) procaspase-3 at the ISL, resulting in two cleavage products: prodomain with large subunit (N+Lg) and small subunit (Sm). No significant cleavage of (B) caspase-3 D175A C163A was observed, verifying that caspase-9 cleaves the ISL of procaspase-3 at D175. Caspase-9 removed the prodomain of (C) procaspase-6 (denoted as ΔN); however, no significant ISL cleavage was observed. (D) The peptide substrate, Ac-LEHD-afc, was employed to measure the LEHD-ase activity of caspase-9. Each experiment (A−D) was performed twice using different samples on two different days, and means ± SD were used to derive the rate constant (k) values. (E) We derived the cleavage rate (k) of caspase-9 to proteolyze the protein substrates, (A) procaspase-3, (B) caspase-3 D175A C163A, and (C) procaspase-6 by plotting $[\ln(1-\rho)/t]$ versus E, where ρ is the percent total band intensity of the ISL cleavage products, t is the time in seconds, and E is the caspase-9 concentration in micromolar. The k values of caspase-9 to cleave the ISL of procaspase-3 and -6 were derived as the negative value of the slope, and for a peptide substrate Ac-LEHD-afc, we reported the cleavage rate (k) as k_{cat}/K_M from panel D.

54−64, 165−185, 201−210, and 251−260) as well as procaspase-6 (1−30, 167−186, and 262−270) were modeled using the UCSF Chimera/MODELER integrated system.[27,28] The illustrations of procaspase-3 and -6 models were created using PyMOL (Schrödinger, LLC).

Sequence Alignment of Procaspase-3 and -6. We used Clustal Omega (https://www.ebi.ac.uk/Tools/msa/clustalo/) to align the sequences of procaspase-3 (Uniprot entry P42574) and procaspase-6 (Uniprot entry P55212).

DNA Plasmids and Generation of Caspase Constructs. Plasmids for expression of wild-type caspase-3 (pET23b-Casp3-His) and wild-type caspase-9 (pET23b-Casp9-His) were gifts from G. Salvesen and obtained from Addgene as plasmids 11821 and 11829, respectively.[29,30] An *E. coli* codon-optimized wild-type caspase-6 gene (with a six-His tag at the C-terminus) was synthetically produced (Celtek Bioscience) and ligated into the NdeI/BamHI sites of the pET11a vector. Wild-type caspase-3 and wild-type caspase-6 plasmids were used as templates to generate their respective constructs (substitutions and deletions) employing QuikChange mutagenesis (Agilent Technologies).

Expression and Purification of Recombinant Caspase Constructs. DNA plasmids for expression of caspase constructs were transformed into the BL21 (DE3) T7 express strain of *E. coli* (New England Biolabs). A single colony was picked for each construct, and overnight seed cultures were grown in 50 mL of LB medium (Research Products International) supplemented with 0.1 mg/mL ampicillin (Fisher BioReagents) by incubation at 37 °C. For large-scale growth, 3 mL of the seed culture of each caspase construct was transferred into 1 L of LB medium containing 0.1 mg/mL ampicillin. Incubation at 37 °C was carried until the desired Abs_{600} (0.6 for caspase-3 constructs, 0.8 for caspase-6 constructs, and 1.0 for caspase-9) was achieved. In each case, protein expression was induced by adding 1 mM IPTG (GoldBio), and the temperatures were decreased (30 °C for caspase-3 constructs, 25 °C for caspase-6 constructs, and 25 °C for caspase-9). After 4 h, cells were centrifuged at 5000 rcf for 7 min at 4 °C, and cell pellets were collected and stored at −80 °C until they were thawed and used for purification.

https://doi.org/10.1021/acs.biochem.1c00459
Biochemistry 2021, 60, 2824−2835

To purify all caspase constructs, we employed Ni^{2+}-ion affinity chromatography followed by anion exchange. Caspase-3 constructs were purified as previously described via the wild-type caspase-3 purification protocol.[31] Caspase-6 constructs were purified as previously described via the procaspase-6 (caspse-6 C163S) purification protocol.[32] Caspase-9 was purified as previously described via the caspase-9 full-length purification protocol.[31] The purity and concentrations of purified caspases were assessed by sodium dodecyl sulfate−polyacrylamide gel electrophoresis (SDS−PAGE), and aliquots were stored at −80 °C until further usage for different assays.

Protein Substrate Digestion and Determination of the Cleavage Rate (*k*). Different concentrations (0, 0.125, 0.25, 0.5, and 1 μM) of caspase-9 were individually incubated with 3 μM individual caspase-3 or -6 construct in an activity assay buffer [100 mM MES (pH 6.5), 20% PEG 400, and 5 mM DTT] for 1 h at 37 °C. Each reaction was stopped by adding 1× SDS loading dye (New England Biolabs). These samples were denatured at 90 °C for 10 min. Each sample was analyzed using 16% SDS−PAGE. SDS−PAGE gels were imaged using a ChemiDocTM MP imaging system (Bio-Rad Laboratories). Band intensities were quantified using Image Lab software (Bio-Rad Laboratories). The cleavage rates of caspase-9 to proteolyze each of the caspase-3 and -6 constructs were determined by following the previously described method.[33,34]

Caspase-9 LEHD-ase Activity and Determination of Kinetic Parameters. We followed the previously described protocol to derive the LEHD-ase activity of caspase-9.[31] For a substrate titration, 10 μL of fluorogenic substrate Ac-LEHD-afc [*N*-acetyl-Leu-Glu-His-Asp-7-amido-4-trifluoromethylcoumarin (Enzo Life Sciences, Inc.)] with concentrations ranging from 0 to 3000 μM was placed in a 96-well black plate. Recombinant caspase-9 (90 μL of an 800 nM solution) in activity assay buffer [100 mM MES (pH 6.5), 20% PEG 400, and 5 mM DTT] was added to each well to achieve a final volume of 100 μL. Immediately, fluorescence kinetics were measured (λ_{ex} = 400 nm, and λ_{em} = 505 nm) at 37 °C for 7 min using a microplate reader (SpectraMax M5, Molecular Devices). Initial velocities versus substrate concentrations were plotted to a Michaelis−Menten curve using GraphPad Prism, and K_M was determined. To derive the exact concentration of caspase-9, an active site titration was performed using a covalent inhibitor, z-VAD-fmk [carbobenzoxy-Val-Ala-Asp-fluoromethylketone (Enzo Life Sciences, Inc.)]. For that, 2 μL of z-VAD-fmk (diluted in DMSO) with the concentrations ranging from 0 to 2 mM was added to a 96-black-well plate containing 90 μL of 800 nM caspase-9 in activity assay buffer. The plate was sealed using aluminum foil and incubated at 25 °C for 1.5 h. Each aliquot (92 μL) was transferred in a duplicate 96-black-well plate containing 1 mM Ac-LEHD-afc (to make 100 μL as a total volume), and fluorescence kinetics were measured using a microplate reader as done for substrate titration. The exact concentration of caspase-9 (total enzyme concentration, E_T) was determined as the lowest concentration at which full inhibition was observed, and using this value, k_{cat} was calculated. Finally, caspase-9 LEHD-ase activity (k_{cat}/K_M) was calculated. The substrate titration and active site titration assays were performed twice using two different aliquots on two separate days.

Generation of Structural Models of Caspase-9 Active Site Accommodating Peptide Substrates. To generate models of the caspase-9 active site bound to peptides, IETD, DVVD, and TEVD as P4−P1 positions, we employed a crystal structure of caspase-9 bound to a peptide substrate, z-EVD-Dcbmk (benzoxycarbonyl-Glu-Val-Asp-dichlorobenzylmethylketone) (PDB entry 1JXQ). We used the mutagenesis feature of PyMOL (Schrödinger, LLC) to substitute the relevant residues. Rotamers of each substituted residue with the minimal clashes were selected to generate models.

RESULTS

Caspase-9 Cleaves the ISL of Procaspase-3 but Not Procaspase-6. To examine the behavior of procaspase-3 and -6 as substrates of wild-type caspase-9 *in vitro*, we performed an SDS-PAGE-based substrate digestion assay. Caspase-9 cleaved caspase-3 C163A (Figure 2A); however, it was unable to proteolyze caspase-3 C163A D175A (Figure 2B). Thus, caspase-9 cleaved procaspase-3 ISL at D175, resulting in two cleavage products: prodomain with large subunit (N+Lg) and small subunit (Sm) (Figure 2A). Caspase-9 cleaved the prodomain of caspase-6 C163S, resulting in caspase-6 ΔN C163S; nevertheless, no significant ISL cleavage was observed (Figure 2C). A previous study showed[35] that removal of the prodomain while the ISL remained intact was not sufficient to achieve procaspase-6 activation. Thus, caspase-9 cannot activate procaspase-6 directly (Figure 2C). From a peptide-based profiling study,[5] the caspase-9 canonical recognition sequence is LEHD (P4−P1). Therefore, we carried out an LEHD-ase activity assay to determine the kinetic parameters (k_{cat} and K_M) of caspase-9 using a fluorogenic peptide substrate Ac-LEHD-afc (Figure 2D). The catalytic efficiency, k (k_{cat}/K_M), of caspase-9 to hydrolyze Ac-LEHD-afc is $(12.8 \pm 1.1) \times 10^4$ μM^{-1} s^{-1} (Figure 2E). For the experiments (Figure 2A−C), the substrate (caspase-3 or -6) concentration (3 μM) was in excess over the enzyme (caspase-9) concentration (0−1 μM). Limitations of the slow kinetics of caspase-9 coupled with the sensitivity of detecting cleaved products make it impossible to monitor the reaction under pseudo-first-order conditions as has been described previously.[33,34] Nevertheless, we used a similar approach[34] to estimate a relative rate (k) for caspase-9 cleavage of the ISLs of procaspase-3, caspase-3 D175A C163A, and procaspase-6 (Figure 2E). These apparent relative cleavage rates (k) for proteolysis of the ISL of procaspase-3, caspase-3 D175A C163A, and procaspase-6 by caspase-9 were 390 ± 30, <25, and <25 M^{-1} s^{-1}, respectively (Figure 2E). The sample calculation of estimating the rate (k) value of caspase-9 to cleave procaspase-3 (in M^{-1} s^{-1}) is shown (Supporting Information xlsx file). We used the same approach throughout this work to approximate rate (k) values. Our results complemented previous findings by various research groups demonstrating caspase-9 does not directly activate procaspase-6.[22−24,36] If its prodomain and the ISL are excluded, procaspase-6 is ∼43% identical in protein sequence to procaspase-3 (Figure S1). Due to the fact that they are the most divergent segments of caspase-6, we hypothesized that the prodomain and/or the ISL of procaspase-6 might protect direct activation of procaspase-6 by caspase-9.

The Prodomain of Procaspase-6 Does Not Play a Significant Role in Protecting Direct Activation by Caspase-9. To test the hypothesis that the procaspase-6 prodomain might protect the procaspase-6 ISL from cleavage, we used caspase-6 ΔN C163S, an uncleaved form of caspase-6 lacking the prodomain. If the prodomain prevents procapase-6 ISL cleavage by caspase-9, then we should observe more ISL cleavage for caspase-6 ΔN C163S than what we observed for caspase-6 C163S (Figure 2C). The ISL cleavage of caspase-6 ΔN C163S by caspase-9 was almost undetectable (Figure 3A). From the comparison, we observed no significant difference in

https://doi.org/10.1021/acs.biochem.1c00459
Biochemistry 2021, 60, 2824−2835

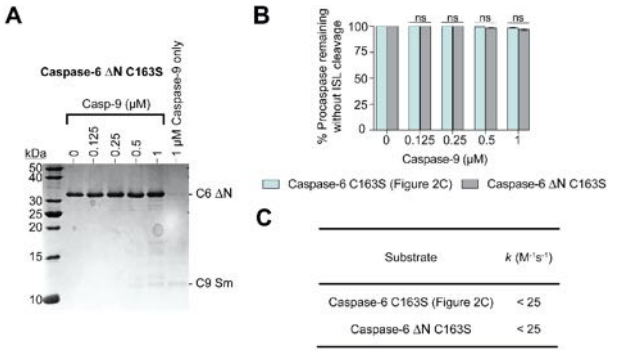

Figure 3. Prodomain of procaspase-6 that does not play a significant role in protecting the ISL from direct activation by caspase-9. (A) Caspase-6 ΔN C163S (3 μM) was incubated with concentrations of caspase-9 ranging from 0 to 1 μM for 1 h at 37 °C. No significant ISL cleavage was observed. (B) Comparison of ISL cleavage between procaspase-6 (Figure 2C) and caspase-6 ΔN C163S by caspase-9. Each experiment was performed twice on two separate days using different samples. The means ± SD of these two replicates were used for statistical analysis using an unpaired two-tailed t test. The p value parameters are denotes with ns (not significant) for $p \geq 0.05$ and one asterisk for $p < 0.05$. No significant difference (shown as ns) in the ISL cleavage was observed between the two constructs for all caspase-9 concentrations. (C) Kinetic rates (k) of caspase-9 to cleave the ISL of procaspase-6 and caspase-6 ΔN C163S were derived as described in the legend of Figure 2.

the ISL cleavage of caspase-6 C163S as compared to caspase-6 ΔN C163S cleavage by caspase-9 (Figure 3B). The estimated rate (k) values for the cleavage of the ISL of both constructs by caspase-9 were <25 M^{-1} s^{-1} (Figure 3C). These data imply that the prodomain does not play a significant role in preventing cleavage of the procaspase-6 ISL by caspase-9. This suggests that the procaspase-6 ISL cleavage sites (site 1, ^{176}DVVD↓N; site 2, ^{190}TEVD↓A) may contribute to substrate selection and should be tested individually.

Caspase-9 Does Not Recognize Procaspase-6 ISL Site 1 (^{176}DVVD↓N). Using sequence alignment, we compared procaspase-6 ISL site 1 (^{176}DVVD↓N) with the procaspase-3 ISL site (^{172}IETD↓S) (Figure 4A). To understand the inability of caspase-9 to hydrolyze procaspase-6 ISL site 1, we engineered a construct in which we introduced the site 1 sequence from procaspase-6 into caspase-3 to generate caspase-3 C163A ^{172}IETD↓S to DVVDN. Using this construct, we asked whether the DVVDN sequence could be cleaved by caspase-9 if it was presented in the background of procaspase-3. We also engineered another construct by introducing the procaspase-3 ISL site into procaspase-6, caspase-6 C163S ^{176}DVVD↓N to IETDS. Using this construct, we can determine whether caspase-9 can recognize an appropriate procaspase-3 cleavage site sequence in the context of procaspase-6. Caspase-9 did not proteolyze caspase-3 C163A ^{172}IETD↓S to DVVDN (Figure 4B), suggesting that the sequence DVVDN is not optimized for cleavage by caspase-9. In contrast, caspase-9 can cleave the ISL of caspase-6 C163S ^{176}DVVD↓N to IETDS, resulting in the generation of cleavage products: Lg and small subunit with intersubunit linker (Sm+ISL) (Figure 4C). This indicated that the context of the region of residues 176−180 is available to caspase-9 for recognition. A previous peptide-based profiling study[5] demonstrated that the most preferred peptide substrate sequence of caspase-9 is LEHD↓ (P4−P1). Therefore, we constructed a third construct, caspase-6 C163S ^{176}DVVD↓N to LEHDS, to analyze how efficiently caspase-9 can proteolyze the canonical consensus sequence. This construct was cleaved at the ISL by caspase-9, resulting in the formation of Lg and Sm+ISL (Figure 4D). No significant difference in the ISL cleavage was detected between caspase-6 C163S and caspase-3 C163A ^{172}IETD↓S to DVVDN (Figure 4E). The rate of cleavage (k) of caspase-9 to proteolyze the ISL of caspase-3 C163A ^{172}IETD↓S to DVVDN was <25 M^{-1} s^{-1} (Figure 4F). Thus, it appears that the caspase-9 active site is unable to recognize the sequence of procaspase-6 ISL site 1, ^{176}DVVD↓N. There was a significant difference in the ISL cleavage when procaspase-6 site 1 was replaced from ^{176}DVVD↓N to IETD/LEHD (Figure 4E). We did not observe significant changes in the ISL cleavage among the constructs, caspase-3 C163A, caspase-6 C163S ^{176}DVVD↓N to IETDS, and caspase-6 C163S ^{176}DVVD↓N to LEHDS (Figure 4E). Moreover, the ISLs of these three constructs were cleaved by caspase-9 with a similar estimated cleavage rate, k (Figures 2E and 4F). These results demonstrated that the caspase-9 active site can access procaspase-6 ISL site 1; however, the sequence DVVDN (P4−P1′) is unfavorable for proteolytic cleavage.

Caspase-9 Does Not Cleave Procaspase-6 ISL Site 2, ^{190}TEVD↓A, Mainly Due to the Local Context. We compared the procaspase-3 ISL site (^{172}IETD↓S) and procaspase-6 ISL site 2 (^{190}TEVD↓A) by aligning the sequences (Figure 5A). To investigate why caspase-9 does not cleave procaspase-6 ISL site 2, which is the sequence first recognized by caspase-6,[25] we engineered constructs caspase-3 C163A ^{172}IETD↓S to TEVDA, caspase-6 C163S ^{190}TEVD↓A to IETDS, and caspase-6 C163S ^{190}TEVD↓A to LEHDS (the canonical caspase-9 recognition motif[5]). Caspase-9 cleaved the ISL of caspase-3 C163A ^{172}IETD↓S to TEVDA, resulting in the formation of cleavage products: N+Lg and Sm (Figure 5B). Although we see a band indicating removal of the prodomain (ΔN), the ISL cleavages for caspase-6 C163S ^{190}TEVD↓A to IETDS and caspase-6 C163S ^{190}TEVD↓A to LEHDS were not observed (Figure 5C,D). We observed a significant difference in the ISL cleavage between the constructs, procaspase-6 and caspase-3 C163A ^{172}IETD↓S to TEVDA (Figure 5E). Thus, caspase-9 can recognize procaspase-6 ISL site 2 in the context of the procaspase-3 background. We observed a significant difference in the ISL cleavage between the constructs, caspase-3 C163A and caspase-3 C163A ^{172}IETD↓S to TEVDA (Figure 5E). Caspase-9 cleaved the ISL of procaspase-3 with an efficiency much higher than that of caspase-3 C163A ^{172}IETD↓S to TEVDA (Figures 2E and 5E). Thus, caspase-9 cannot efficiently recognize the sequence of procaspase-6 ISL site 2, ^{190}TEVD↓A, even when it was presented in an optimal context in procaspase-3. No significant change in the ISL cleavage was observed among the constructs: caspase-6 C163S, caspase-6 C163S ^{190}TEVD↓A to IETDS, and caspase-6 C163S ^{190}TEVD↓A to LEHDS (Figure 5E). The rates, k, of cleavage of the ISLs of these three constructs by caspase-9 were <25 M^{-1} s^{-1} (Figures 2E and 5F). Thus, even replacing procaspase-6 ISL site 2 (^{190}TEVD↓A) with IETDS or LEHDS (the most preferred sequence of the caspase-9 active site for P4−P1 positions[5]) resulted in almost no ISL cleavage. These results strongly suggest that in addition to the sequence, the local context of procaspase-6 ISL site 2 (^{190}TEVD↓A) plays a vital role in blocking the access of caspase-9.

The Caspase-9 Active Site Preference for P4−P1′ Positions Is IETDS > TEVDA > DVVDN. We used a previously

https://doi.org/10.1021/acs.biochem.1c00459
Biochemistry 2021, 60, 2824−2835

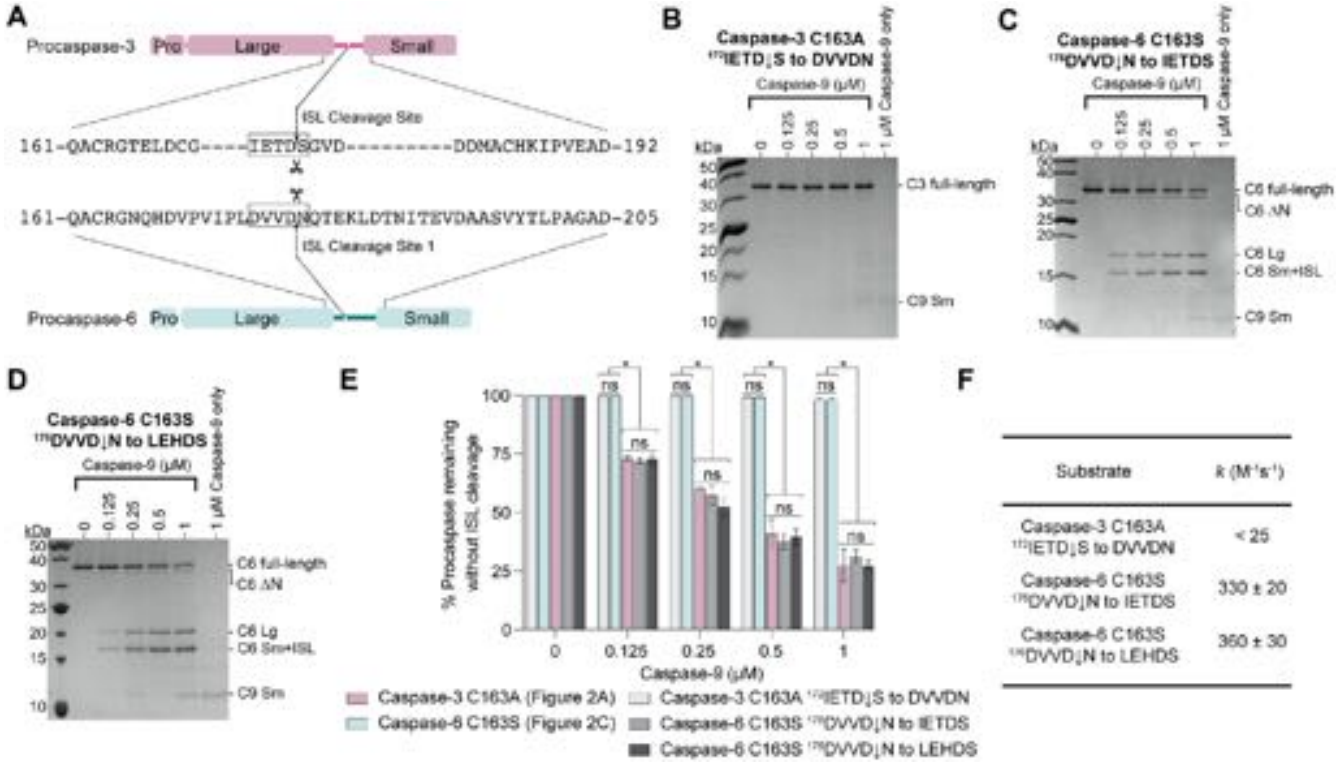

Figure 4. Caspase-9 does not recognize the sequence of procaspase-6 ISL site 1, ^{176}DVVD↓N. (A) Sequence alignment of the ISL of procaspase-3 and -6. The ISL site of procaspase-3 (^{172}IETD↓S) and ISL site 1 of procaspase-6 (^{176}DVVD↓N) are shown in boxes. (B–D) Different concentrations of recombinant caspase-9 ranging from 0 to 1 μM were incubated with 3 μM caspase-3 C163A ^{172}IETD↓S to DVVDN, caspase-6 C163S ^{176}DVVD↓N to IETDS, and caspase-6 C163S ^{176}DVVD↓N to LEHDS, respectively, for 1 h at 37 °C. In the last lane of each gel, 1 μM caspase-9 alone was loaded as a control. Caspase-9 could cleave the ISL of (B) caspase-3 C163A IETDS to DVVDN. In contrast, caspase-9 cleaved the ISL for (C) caspase-6 C163S ^{176}DVVD↓N to IETDS and (D) caspase-6 C163S ^{176}DVVD↓N to LEHDS, resulting in Lg and small subunit with intersubunit linker (Sm+ISL). (E) Comparison of ISL cleavage among different constructs of caspase-3 and -6 by caspase-9. No significant difference was observed between ISL cleavage of procaspase-6 (Figure 2C) and caspase-3 C163A IETDS to DVVDN. No significant difference was observed among ISL cleavage of procaspase-3 (Figure 2A) and caspase-6 C163S DVVDN to IETDS/LEHDS. Each experiment (B–D) was performed twice on two different days using different samples. The means ± SD of the two replicates were used to perform statistical analysis using the unpaired two-tailed *t* test as parameters defined in Figure 3B, where ns denotes $p \geq 0.05$ and one asterisk denotes $p < 0.05$. For *t* test analysis, we compared each construct with the other four constructs individually. (F) Rate (*k*, as defined in Figure 2) of cleavage of ISL sequence constructs of caspase-3 and -6 by caspase-9.

determined crystal structure (PDB entry 1JXQ) to model the caspase-9 active site bound to different peptides.[37] This reported crystal structure has a peptide-based inhibitor, z-EVD-Dcbmk (benzoxycarbonyl-Glu-Val-Asp-dichlorobenzylmethylketone), bound at the active site pocket occupying the P4–P1 positions (Figure 6A). Using the mutagenesis feature of PyMOL, we generated structural models of binding of the caspase-9 active site to peptides IETD, TEVD, and DVVD (panels B–D respectively, of Figure 6). The S4 subsite of the caspase-9 active site contains residues I396, Y397, W354, and W362, rendering it hydrophobic. Therefore, isoleucine, a hydrophobic residue, can be accommodated at the P4 position (Figure 6B). Aspartic acid present in DVVDN is a very hydrophilic residue that may resist residing inside the S4 subsite (Figure 6C). Moreover, the presence of D356 near the S4 subsite may further decrease the affinity for a negatively charged aspartic acid at the P4 position (Figure 6C). Threonine is uncharged and less hydrophilic than aspartic acid. Thus, the S4 subsite may more readily accept threonine (Figure 6D). Peptides IETD and TEVD have the advantage of possessing glutamic acid as the P3 position, which can interact with R355 via hydrogen bonding (Figure 6B,D). In contrast, valine, a hydrophobic residue, is not suitable for S3 subsite binding (Figure 6C). The threonine of the IETD peptide can interact with K292 by making a hydrogen bond (Figure 6B). Upon examination of the cavity of the S1′ subsite, small residues such as glycine, serine, and alanine are more preferred than asparagine as the P1′ position [not shown in the figure because position P1′ was not present in the original structure (Figure 6A)]. Therefore, the caspase-9 active site preference for the P4–P1′ positions is IETDS > TEVDA > DVVDN. Calculation of the solvent accessible surface area (SASA) also provides insights into recognition preferences (Table S1). While the cleavage site in procaspase-3 and site 1 in procaspase-6 are both highly accessible, site 2 in procaspase-6 is much less accessible. The structural models (Figure 6) and SASA analysis support our cleavage assay data that caspase-9 (i) cleaves the procaspase-3 ISL site (^{172}IETD↓S) with a higher cleavage rate (Figure 2), (ii) does not recognize procaspase-6 ISL site 1 (^{176}DVVD↓N) (Figure 4), and (iii) can cleave the sequence of procaspase-6 ISL site 2, ^{190}TEVD↓A, with a lower cleavage rate (Figure 5) and (iv) procaspase-6 site 2 is buried by the local context that play an important role in preventing the cleavage by caspase-9.

■ DISCUSSION

The order of caspase activation during the intrinsic apoptotic pathway has been studied in depth previously.[22,38] On the basis of these studies, we created a schematic diagram of intrinsic apoptosis focusing on caspase-9 activation via the apoptosome

https://doi.org/10.1021/acs.biochem.1c00459
Biochemistry 2021, 60, 2824–2835

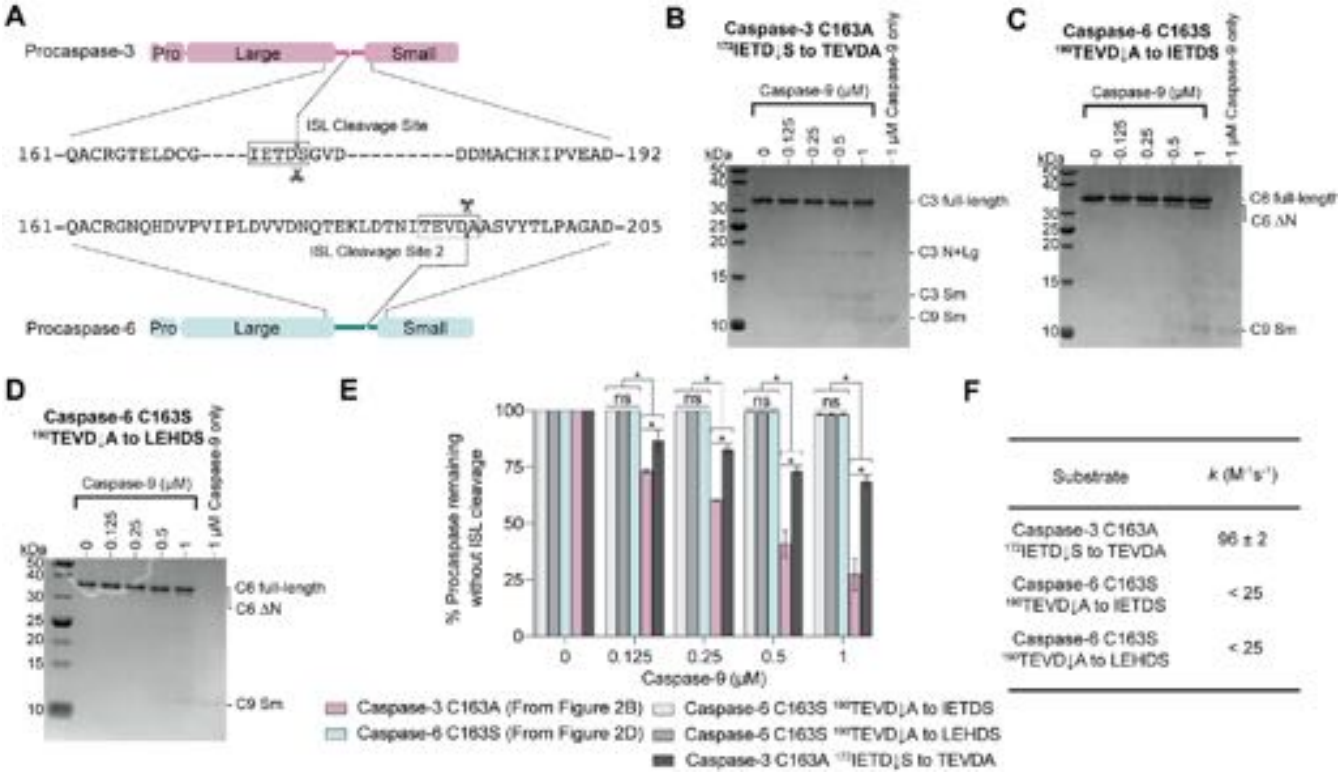

Figure 5. Caspase-9 does not cleave procaspase-6 ISL site 2, ^{190}TEVD↓A, mainly due to the local context. (A) Sequence alignment of the ISL of procaspase-3 and -6. The ISL site of procaspase-3 (^{172}IETD↓S) and ISL site 2 of procaspase-6 (^{190}TEVD↓A) are shown in boxes. (B–D) Recombinant caspase-9 ranging from 0 to 1 μM was incubated with 3 μM caspase-3 C163A ^{172}IETD↓S to TEVDA, caspase-6 C163S ^{190}TEVD↓A to IETDS, and caspase-6 C163S ^{190}TEVD↓A to LEHDS, respectively, for 1 h at 37 °C. In the last lane of each gel, 1 μM caspase-9 was loaded as a control. We observe the ISL cleavage of (B) caspase-3 C163A ^{172}IETD↓S to TEVDA, indicating that TEVDA can be recognized by caspase-9. The ISL cleavage of (C) caspase-6 ^{190}TEVD↓A to IETDS and (D) caspase-6 ^{190}TEVD↓A to LEHDS was too low to be detected. (E) Comparison of the ISL cleavage among different constructs of caspase-3 and -6 by caspase-9. No significant difference was observed between ISL cleavage of procaspase-6 and caspase-6 C163A ^{190}TEVD↓A to IETDS/LEHDS. Replacing the ISL site of procaspase-3 from ^{172}IETD↓S to TEVDA resulted in significantly less ISL cleavage compared to procaspase-3 (Figure 2A). Each experiment (B–D) was performed twice on two different days using different samples. The means ± SD of the two replicates were used to perform statistical analysis via an unpaired two-tailed *t* test as defined in the legends of Figures 3C and 4E, where ns denotes $p \geq 0.05$ and one asterisk denotes $p < 0.05$. For the *t* test analysis, each construct was compared with the other four constructs individually. (F) Rate (*k*, as defined in Figure 2) of cleavage of different constructs of caspase-3 and -6 by caspase-9.

complex and the order of activation of the executioners (caspase-3, -6, and -7) (Figure 7A). Once triggered via formation of the apoptosome, caspase-9 mediates the activation of procaspase-3 and -7. In the case of procaspase-3, caspase-9 cuts the ISL site (^{172}IETD↓S) (Figure 2A,B). This proteolytic cleavage event at the ISL is required to activate procaspase-3[39,40] (Figure 7B). After this ISL cleavage, to achieve complete maturation, the prodomain of caspase-3 is removed (first cleavage at D9 and then at D28) likely via self-proteolysis or caspase-3-like activity.[41,42] Activated caspase-3 further processes caspase-9 via a feedback mechanism, a cleavage event at D330[22] (Figure 7A). Procaspase-7 contains three cleavage sites: D23, D198, and D206.[43] To activate procaspase-7, prodomain (residues 1–23)[44] and then N-terminal peptide (residues 23–28)[45] are removed, perhaps by active caspase-3. These cleavage events facilitate procaspase-7 activation via ISL cleavage by initiator caspases (e.g., caspase-9 and -8). Caspase-9 activates procaspase-7 (Figure 7A) via cleavage at ISL site 1 (^{195}IQAD↓S) and ISL site 2 (^{203}NDTD↓A).[45] The rates (*k*) for caspase-9 to cut procaspase-7 ISL site 1 (^{195}IQAD↓S) and ISL site 2 (^{203}NDTD↓A) were determined to be $\sim 0.4 \times 10^4$ and <200 M^{-1} s^{-1}, respectively.[33] Thus, caspase-9 proteolyzes procaspase-7 ISL site 1 with a much higher cleavage rate than it does ISL site 2. Swapping the procaspase-7 ISL site 2 from ^{203}NDTD↓A to LEHDA robustly enhanced the cleavage rate of caspase-9 (from <200 to $\sim 0.1 \times 10^4$ M^{-1} s^{-1}),[33] exemplifying the importance of the cleavage site motif sequence in proteolysis. Nevertheless, this improved cleavage rate of caspase-9 for this swapped construct of procaspase-7 was ~4 times lower than the cleavage rate to hydrolyze at ISL site 2, ^{195}IQAD↓S.[33] Thus, ISL site 1 of procaspase-7 appears to be more accessible to the caspase-9 active site than ISL site 2, illustrating the importance of the local context of a cleavage site in the process of proteolysis.

The inability of caspase-9 to directly activate procaspase-6 (Figure 7A) has been reported in previous studies.[22−24,36] Proteolytic cleavage at any of the ISL cleavage sites (at either D179 or D193) of procaspase-6 is a prerequisite to activate procaspase-6.[21,35] Moreover, ISL cleavage of procaspase-6 results in structural-dynamics changes rendering the active site more accessible to solvent.[46] On the basis of our results from this study (Figures 2, 4, and 5), we prepared a schematic diagram showcasing the interactions between caspase-9 and procaspase-6 (Figure 7C). We demonstrate that procaspase-6 ISL site 1 (^{176}DVVD↓N) is accessible (in other words, the local context of this cleavage site is not creating hindrance) to the active site of caspase-9. However, the sequence of this cleavage site (DVVDN as P4–P1′), illustrated as transparent blue spheres for each monomer (Figure 7C), is unrecognizable (Figure 4). We also

https://doi.org/10.1021/acs.biochem.1c00459
Biochemistry 2021, 60, 2824−2835

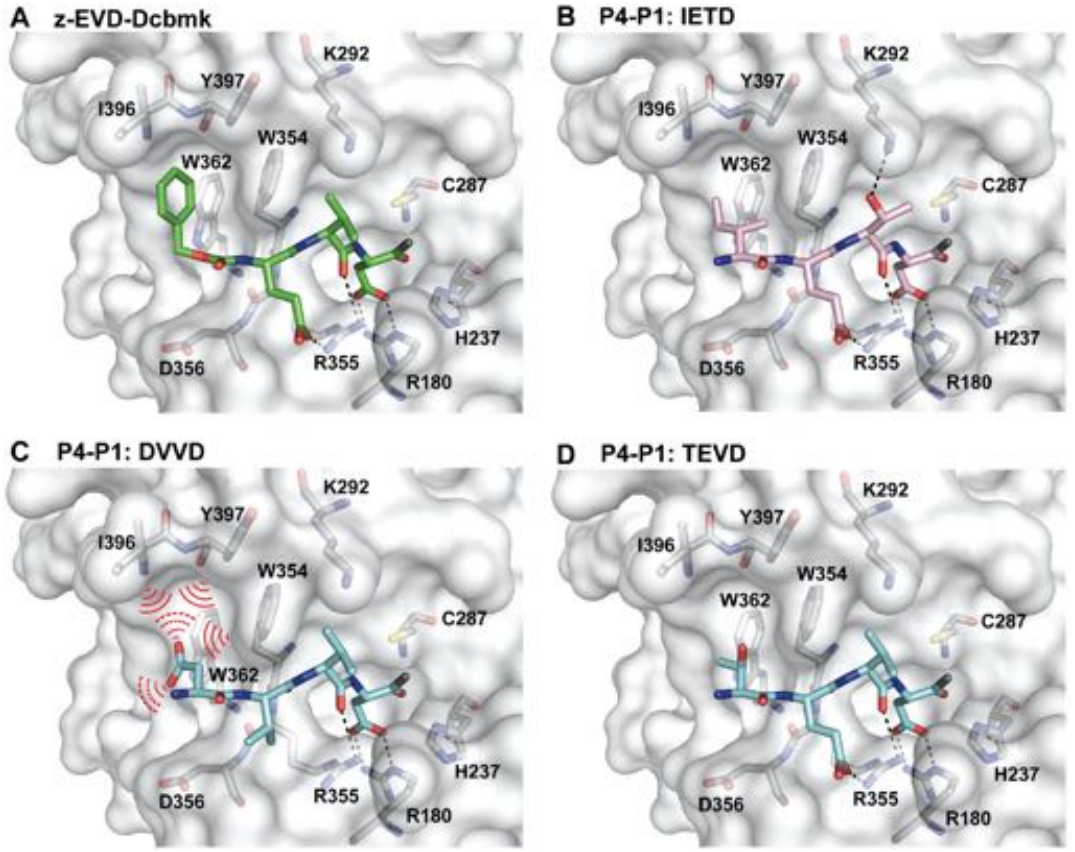

Figure 6. Caspase-9 active site preference for the P4−P1′ positions in the substrate is IETDS > TEVDA > DVVDN. (A−D) Active site of caspase-9 accommodating peptides (A) z-EVD-Dcbmk (benzoxycarbonyl-Glu-Val-Asp-dichlorobenzylmethylketone, PDB entry 1JXQ),[37] (B) IETD, (C) DVVD, and (D) TEVD, respectively, modeled as residues in the P4−P1 positions. IETD, DVVD, and TEVD peptides were generated using the mutagenesis feature of PyMOL. The hydrogen bonds between each peptide residue and caspase-9 active site residues are shown as black dashes. The threonine in (B) the IETD peptide is predicted to make a hydrogen bond with K292. Thus, the P2 position of IETD is more preferred by caspase-9 compared to other peptides in panels A, C, and D. Due to the presence of valine at the P2 position, fewer hydrogen bond interactions with R355 are predicted to form for (C) the DVVD peptide compared to other peptides in panels A, B, and D. The S4 subsite of caspase-9 is hydrophobic, consisting of residues I396, Y397, W354, and W362. Hydrophobic residues at the P4 position in (A) z-EVD-Dcbmk and (B) IETD peptides are preferred; however, aspartate (a very hydrophilic residue) at the P4 position in (C) DVVD peptide is expected to lack enthalpically driven interactions, as illustrated by red clashes.

found that the active site of caspase-9 can recognize the sequence of procaspase-6 site 2 (^{190}TEVD↓A). Nonetheless, the local context of this ISL cleavage site, shown as clashes (Figure 7C), is blocking the access of the caspase-9 active site (Figure 5). Thus, both the sequence and the local context of procaspase-6 ISL cleavage sites play vital roles in preventing direct activation by caspase-9. We observed that caspase-9 only partially cleaved the prodomain of procaspase-6, but not any other sites, although caspase-9 was present at concentrations above those expected physiologically (Figure 2C). The removal of only the prodomain is not sufficient for procaspase-6 activation.[35] Thus, procaspase-6 proteolysis by caspase-9 simply results in an inactive ΔN version of caspase-6 (Figure 7C).

Upon its activation by caspase-9, caspase-3 hydrolyzes procaspase-6 into mature caspase-6[22,23] (Figure 7A). Active caspase-3 proteolyzes procaspase-6 at all three cleavage sites: D23, D179, and D193.[23,25] Among these three cleavage sites of procaspase-6, caspase-3 directly cuts at D23 and D179, and only then can proteolysis at D193 occur.[23,25] These findings strongly suggested that procaspase-6 ISL site 1 (^{176}DVVD↓N) is readily accessible and recognizable to the active site of caspase-3. Moreover, the local context of procaspase-6 ISL site 2 (^{190}TEVD↓A) initially blocks the caspase-3 active site and allows the access only after the prior cleavage event at D179,[23] although is it difficult to disentangle the contribution of a more favorable recognition sequence. Activated caspase-6 can also proteolyze procaspase-6 intermolecularly at all three cleavage sites: D23, D179, and D193.[25] Among these three cleavage sites, active caspase-6 robustly cleaves at D23 but inefficiently proteolyzes at D179 and D193.[23,25] Active caspase-6 was able to hydrolyze procaspase-6 ISL site 1 with a much higher efficiency when the sequence ^{176}DVVD was substituted with TETD (P4−P1 sequence of the procaspase-6 prodomain).[25] Thus, as we determined for caspase-9 (Figure 4), the sequence of procaspase-6 site 1 is not well recognized by caspase-6 via intermolecular recognition. Nevertheless, when it engages in an intermolecular interaction, in contrast to caspase-3, active caspase-6 can cut procaspase-6 at D193 without any need for prior cleavage at D179.[23,25] Thus, unlike active caspase-9 (Figure 5) and caspase-3,[23,25] active caspase-6 can access and directly cleave procaspase-6 ISL site 2 (^{190}TEVD↓A). Despite the fact that caspase-3 hydrolyzes its preferred fluorogenic peptide substrate (DEVD-ase activity)[47] with a k_{cat}/K_M value ∼5-fold higher than that of caspase-6 (VEID-ase activity),[48,49] the inability of caspase-3 and the ability of caspase-6 to directly proteolyze the procaspase-6 ISL site 2 via intermolecular

https://doi.org/10.1021/acs.biochem.1c00459
Biochemistry 2021, 60, 2824−2835

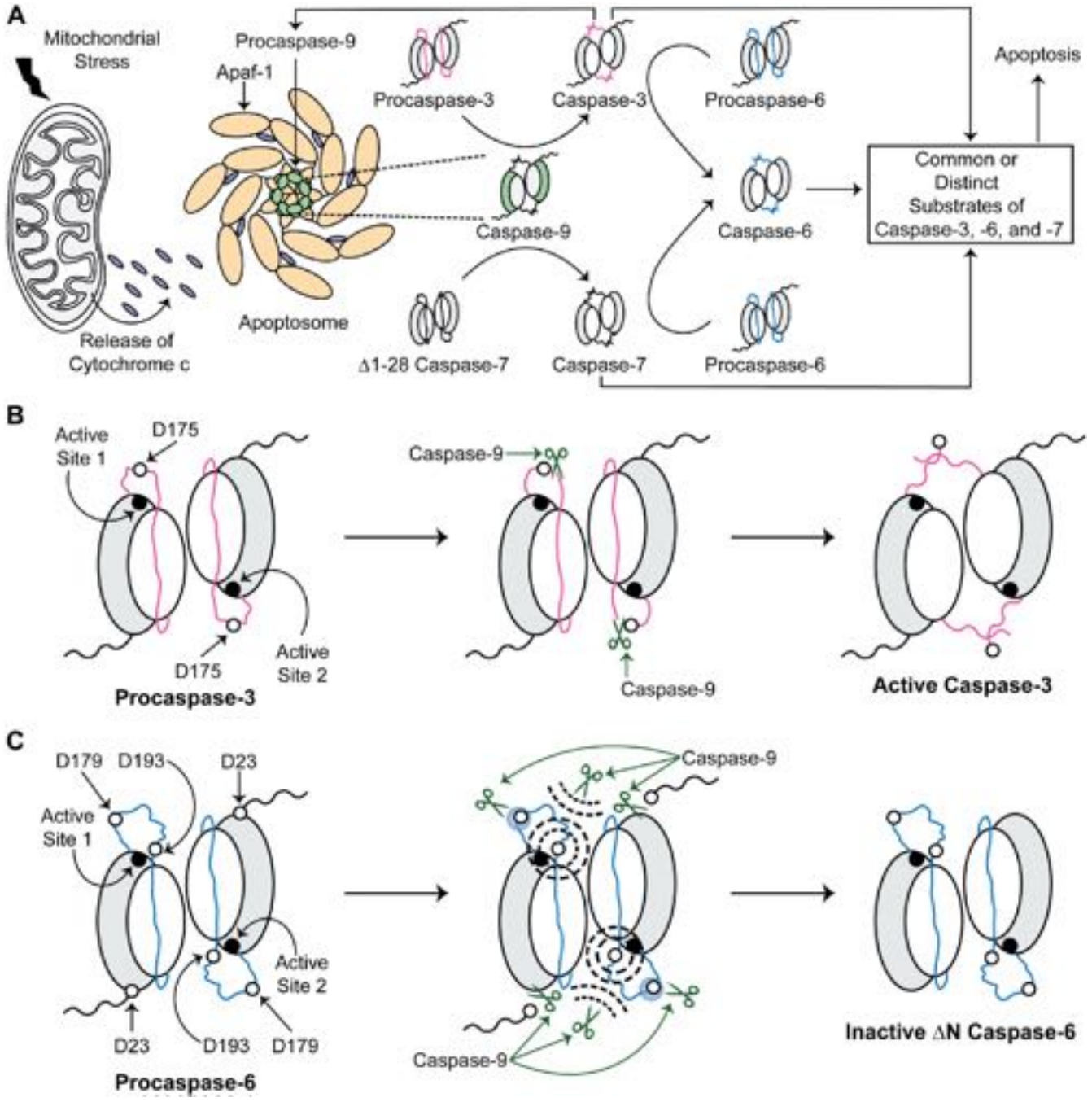

Figure 7. In the intrinsic apoptotic pathway, caspase-9 cannot directly activate caspase-6 due to the sequence of ISL cleavage site 1 and the local context of ISL cleavage site 2. (A) Schematic diagram adapted from the literature illustrating the order of caspase activation during the intrinsic path of apoptosis.[22,38] Mitochondrial stress releases cytochrome *c*, which interacts with Apaf-1 (apoptotic protease activating factor 1, orange), to form the apoptosome complex that recruits procaspase-9 to mediate activation of caspase-9. Caspase-9 then activates caspase-3 and -7; however, it is unable to activate caspase-6 directly. Activated caspase-3 processes procaspase-9 via a feedback mechanism. Caspase-3 also cleaves and activates procaspase-6. In the absence of active caspase-3, activated caspase-7 activates procaspase-6. The apoptotic executioners (caspase-3, -6, and -7) cleave their respective downstream substrates to evoke apoptosis. (B) Schematic diagram showing caspase-9 activating procaspase-3 by ISL cleavage at D175. (C) Schematic diagram showing caspase-9 can access D179 of procaspase-6 but the sequence, DVVDN, is uncleavable (P4−P1′ cleavage sites for each monomer are shown as transparent blue spheres). Caspase-9 is unable to hydrolyze D193 due to the local context (inaccessibility shown as clashes). Though caspase-9 can remove the prodomain of procaspase-6, the resultant product (ΔN caspase-6) is inactive, which cannot hydrolyze downstream substrates.[35]

interactions signify the importance of the local context of cleavage sites in the process of proteolysis. Early work in the field showed that caspase-3 but not caspase-7 activated caspase-6.[50] More recently, in at least one study of the intrinsic apoptotic pathway,[38] in the absence of caspase-3, activated caspase-7 was able to activate procaspase-6 to caspase-6 (Figure 7A); however, the molecular factors facilitating this activation remain to be identified.

Peptide-based screening and proteomics-wide studies of an individual protease are insightful in designing active site inhibitors/peptide substrates[5,26,51] and obtaining the list of protein substrates,[52−54] respectively. However, this information

https://doi.org/10.1021/acs.biochem.1c00459
Biochemistry 2021, 60, 2824−2835

is not sufficent to completely understand the substrate preference of an individual protease. Such knowledge at a molecular level can be determined only by performing biochemical and/or biophysical studies on a protease and its substrates. Interactions between many proteases and their protein substrates (e.g., caspase-9 and the executioners, procaspase-3, -6, and -7) are transient; therefore, deriving the structural information about their complexes using biophysical techniques such as X-ray crystallography, nuclear magnetic resonance, and cryo-electron microscopy is challenging [e.g., currently, there is no structure deposited of a complex of caspase-9 with any of its protein substrates in the Protein Data Bank (https://www.rcsb.org/)]. In such cases, using site-directed mutagenesis coupled with protein substrate digestion assays, as we have undertaken herein, can help in elucidating the mechanisms of biological pathways at a molecular level. This study demonstrates two key points: (i) that the molecular architecture of procaspase-6 renders it insensitive to caspase-9 activation, although its ISL cleavage sites are positioned (within the ISL) like those in procaspase-3/-7, and (ii) that sequence as well as the local context of the cleavage sites enables productive proteolytic activation.

■ ASSOCIATED CONTENT

Supporting Information

The Supporting Information is available free of charge at https://pubs.acs.org/doi/10.1021/acs.biochem.1c00459.

Amino acid sequence alignment of procaspase-3 and -6 with the percent identity of the prodomain, the large subunit, the small subunit, and the intersubunit linker, and SASA calculation of procaspase-3 and -6 intersubunit linker cleavage sites (PDF)

Sample calculation of the derivation of the rate (k) of cleavage of the ISL of caspase-3 C163A by caspase-9 using the raw data of two replicates (XLSX)

Accession Codes

UniprotKB: caspase-3 (CASP3_HUMAN, P42574), caspase-6 (CASP6_HUMAN, P55212), caspase-7 (CASP7_HUMAN, P55210), caspase-8 (CASP8_HUMAN, Q14790), caspase-9 (CASP9_HUMAN, P55211), caspase-10 (CASPA_HUMAN, Q92851), ClpP from *E. coli* (CLPP_ECOLI, P0A6G7), ClpP from *S. aureus* (CLPP_STAAR, Q6GIM3), ClpP from human mitochondria (CLPP_HUMAN, Q16740), ClpP from *C. crescentus* (CLPP_CAUVN, B8GX16), and ClpX from *C. crescentus* (CLPX_CAUVN, B8GX14).

■ AUTHOR INFORMATION

Corresponding Author

Jeanne A. Hardy − *Department of Chemistry and Models to Medicine Center, Institute of Applied Life Sciences, University of Massachusetts, Amherst, Massachusetts 01003, United States;* orcid.org/0000-0002-3406-7997; Email: jhardy@umass.edu

Author

Ishankumar V. Soni − *Department of Chemistry, University of Massachusetts, Amherst, Massachusetts 01003, United States*

Complete contact information is available at: https://pubs.acs.org/10.1021/acs.biochem.1c00459

Funding

This work was supported by the National Institutes of Health (R01 GM 008532). I.V.S. was supported in part by the National Institutes of Health (T32 GM008515).

Notes

The authors declare no competing financial interest.

■ ABBREVIATIONS

P, peptide residues of the substrates; S, subsites of the protease active site; ISL, intersubunit linker; N, N-terminal prodomain; ΔN, lacking the prodomain; Lg, large subunit; Sm, small subunit; Ac-LEHD-afc, *N*-acetyl-Leu-Glu-His-Asp-7-amido-4-trifluoromethylcoumarin; z-EVD-Dcbmk, benzoxycarbonyl-Glu-Val-Asp-dichlorobenzylmethylketone; z-VAD-fmk, carbobenzoxy-Val-Ala-Asp-fluoromethylketone; SASA, solvent accessible surface area; SD, standard deviation.

■ REFERENCES

(1) King, R. W.; Deshaies, R. J.; Peters, J.-M.; Kirschner, M. W. How proteolysis drives the cell cycle. *Science* **1996**, *274*, 1652−1659.

(2) Sordet, O.; Rébé, C.; Plenchette, S.; Zermati, Y.; Hermine, O.; Vainchenker, W.; Garrido, C.; Solary, E.; Dubrez-Daloz, L. Specific involvement of caspases in the differentiation of monocytes into macrophages. *Blood* **2002**, *100*, 4446−4453.

(3) Coll, N. S.; Vercammen, D.; Smidler, A.; Clover, C.; Van Breusegem, F.; Dangl, J. L.; Epple, P. Arabidopsis type I metacaspases control cell death. *Science* **2010**, *330*, 1393−1397.

(4) Schechter, I.; Berger, A. On the size of the active site in proteases. I. Papain. *Biochem. Biophys. Res. Commun.* **1967**, *27*, 157−162.

(5) Thornberry, N. A.; Rano, T. A.; Peterson, E. P.; Rasper, D. M.; Timkey, T.; Garcia-Calvo, M.; Houtzager, V. M.; Nordstrom, P. A.; Roy, S.; Vaillancourt, J. P.; Chapman, K. T.; Nicholson, D. W. A combinatorial approach defines specificities of members of the caspase family and granzyme B. *J. Biol. Chem.* **1997**, *272*, 17907−17911.

(6) Hill, M. E.; MacPherson, D. J.; Wu, P.; Julien, O.; Wells, J. A.; Hardy, J. A. Reprogramming Caspase-7 Specificity by Regio-Specific Mutations and Selection Provides Alternate Solutions for Substrate Recognition. *ACS Chem. Biol.* **2016**, *11*, 1603−1612.

(7) Gersch, M.; Stahl, M.; Poreba, M.; Dahmen, M.; Dziedzic, A.; Drag, M.; Sieber, S. A. Barrel-shaped ClpP Proteases Display Attenuated Cleavage Specificities. *ACS Chem. Biol.* **2016**, *11*, 389−399.

(8) Tremblay, C. Y.; Vass, R. H.; Vachet, R. W.; Chien, P. The Cleavage Profile of Protein Substrates by ClpXP Reveals Deliberate Starts and Pauses. *Biochemistry* **2020**, *59*, 4294−4301.

(9) Ghavami, S.; Hashemi, M.; Ande, S. R.; Yeganeh, B.; Xiao, W.; Eshraghi, M.; Bus, C. J.; Kadkhoda, K.; Wiechec, E.; Halayko, A. J.; Los, M. Apoptosis and cancer: Mutations within caspase genes. *J. Med. Genet.* **2009**, *46*, 497−510.

(10) Olsson, M.; Zhivotovsky, B. Caspases and cancer. *Cell Death Differ.* **2011**, *18*, 1441−1449.

(11) Puck, J. M.; Zhu, S. Immune disorders caused by defects in the caspase cascade. *Curr. Allergy Asthma Rep.* **2003**, *3*, 378−384.

(12) Furlan, R.; Martino, G.; Galbiati, F.; Poliani, P. L.; Smiroldo, S.; Bergami, A.; Desina, G.; Comi, G.; Flavell, R.; Su, M. S.; Adorini, L. Caspase-1 regulates the inflammatory process leading to autoimmune demyelination. *J. Immunol.* **1999**, *163*, 2403−2409.

(13) Wang, X.-J.; Cao, Q.; Zhang, Y.; Su, X.-D. Activation and Regulation of Caspase-6 and Its Role in Neurodegenerative Diseases. *Annu. Rev. Pharmacol. Toxicol.* **2015**, *55*, 553−572.

(14) Graham, R. K.; Ehrnhoefer, D. E.; Hayden, M. R. Caspase-6 and neurodegeneration. *Trends Neurosci.* **2011**, *34*, 646−656.

(15) Moretti, A.; Weig, H.-J.; Ott, T.; Seyfarth, M.; Holthoff, H.-P.; Grewe, D.; Gillitzer, A.; Bott-Flügel, L.; Schömig, A.; Ungerer, M.; Laugwitz, K.-L. Essential myosin light chain as a target for caspase-3 in failing myocardium. *Proc. Natl. Acad. Sci. U. S. A.* **2002**, *99*, 11860−11865.

(16) Seaman, J. E.; Julien, O.; Lee, P. S.; Rettenmaier, T. J.; Thomsen, N. D.; Wells, J. A. Cacidases: Caspases can cleave after aspartate, glutamate and phosphoserine residues. *Cell Death Differ.* **2016**, *23*, 1717−1726.
(17) Li, Y.; Zhou, M.; Hu, Q.; Bai, X.-c.; Huang, W.; Scheres, S. H. W.; Shi, Y. Mechanistic insights into caspase-9 activation by the structure of the apoptosome holoenzyme. *Proc. Natl. Acad. Sci. U. S. A.* **2017**, *114*, 1542−1547.
(18) Fu, T.-M.; Li, Y.; Lu, A.; Li, Z.; Vajjhala, P. R.; Cruz, A. C.; Srivastava, D. B.; DiMaio, F.; Penczek, P. A.; Siegel, R. M.; Stacey, K. J.; Egelman, E. H.; Wu, H. Cryo-EM Structure of Caspase-8 Tandem DED Filament Reveals Assembly and Regulation Mechanisms of the Death-Inducing Signaling Complex. *Mol. Cell* **2016**, *64*, 236−250.
(19) Nicholson, D. W.; Ali, A.; Thornberry, N. A.; Vaillancourt, J. P.; Ding, C. K.; Gallant, M.; Gareau, Y.; Griffin, P. R.; Labelle, M.; Lazebnik, Y. A.; Munday, N. A.; Raju, S. M.; Smulson, M. E.; Yamin, T.-T.; Yu, V. L.; Miller, D. K. Identification and inhibition of the ICE/CED-3 protease necessary for mammalian apoptosis. *Nature* **1995**, *376*, 37−43.
(20) Fernandes-Alnemri, T.; Armstrong, R. C.; Krebs, J.; Srinivasula, S. M.; Wang, L.; Bullrich, F.; Fritz, L. C.; Trapani, J. A.; Tomaselli, K. J.; Litwack, G.; Alnemri, E. S. In vitro activation of CPP32 and Mch3 by Mch4, a novel human apoptotic cysteine protease containing two FADD-like domains. *Proc. Natl. Acad. Sci. U. S. A.* **1996**, *93*, 7464−7469.
(21) Vaidya, S.; Velázquez-Delgado, E. M.; Abbruzzese, G.; Hardy, J. A. Substrate-induced conformational changes occur in all cleaved forms of caspase-6. *J. Mol. Biol.* **2011**, *406*, 75−91.
(22) Slee, E. A.; Harte, M. T.; Kluck, R. M.; Wolf, B. B.; Casiano, C. A.; Newmeyer, D. D.; Wang, H.-G.; Reed, J. C.; Nicholson, D. W.; Alnemri, E. S.; Green, D. R.; Martin, S. J. Ordering the Cytochrome c-initiated Caspase Cascade: Hierarchical Activation of Caspases-2, −3, −6, −7, −8, and −10 in a Caspase-9-dependent Manner. *J. Cell Biol.* **1999**, *144*, 281−292.
(23) Simon, D. J.; Weimer, R. M.; McLaughlin, T.; Kallop, D.; Stanger, K.; Yang, J.; O'Leary, D. D. M.; Hannoush, R. N.; Tessier-Lavigne, M. A caspase cascade regulating developmental axon degeneration. *J. Neurosci.* **2012**, *32*, 17540−17553.
(24) McComb, S.; Chan, P. K.; Guinot, A.; Hartmannsdottir, H.; Jenni, S.; Dobay, M. P.; Bourquin, J.-P.; Bornhauser, B. C. Efficient apoptosis requires feedback amplification of upstream apoptotic signals by effector caspase-3 or −7. *Sci. Adv.* **2019**, *5*, eaau9433.
(25) Wang, X.-J.; Cao, Q.; Liu, X.; Wang, K.-T.; Mi, W.; Zhang, Y.; Li, L.-F.; LeBlanc, A. C.; Su, X.-D. Crystal structures of human caspase 6 reveal a new mechanism for intramolecular cleavage self-activation. *EMBO Rep.* **2010**, *11*, 841−847.
(26) Thomsen, N. D.; Koerber, J. T.; Wells, J. A. Structural snapshots reveal distinct mechanisms of procaspase-3 and −7 activation. *Proc. Natl. Acad. Sci. U. S. A.* **2013**, *110*, 8477−8482.
(27) Webb, B.; Sali, A. Protein structure modeling with MODELLER. *Methods Mol. Biol.* **2014**, *1137*, 1−15.
(28) Pettersen, E. F.; Goddard, T. D.; Huang, C. C.; Couch, G. S.; Greenblatt, D. M.; Meng, E. C.; Ferrin, T. E. UCSF Chimera - A visualization system for exploratory research and analysis. *J. Comput. Chem.* **2004**, *25*, 1605−1612.
(29) Zhou, Q.; Snipas, S.; Orth, K.; Muzio, M.; Dixit, V. M.; Salvesen, G. S. Target protease specificity of the viral serpin CrmA. Analysis of five cascapses. *J. Biol. Chem.* **1997**, *272*, 7797−7800.
(30) Stennicke, H. R.; Deveraux, Q. L.; Humke, E. W.; Reed, J. C.; Dixit, V. M.; Salvesen, G. S. Caspase-9 can be activated without proteolytic processing. *J. Biol. Chem.* **1999**, *274*, 8359−8362.
(31) Huber, K. L.; Serrano, B. P.; Hardy, J. A. Caspase-9 CARD: Core domain interactions require a properly formed active site. *Biochem. J.* **2018**, *475*, 1177−1196.
(32) Okerberg, E. S.; Dagbay, K. B.; Green, J. L.; Soni, I.; Aban, A.; Nomanbhoy, T. K.; Savinov, S. N.; Hardy, J. A.; Kozarich, J. W. Chemoproteomics Using Nucleotide Acyl Phosphates Reveals an ATP Binding Site at the Dimer Interface of Procaspase-6. *Biochemistry* **2019**, *58*, 5320−5328.
(33) Boucher, D.; Blais, V.; Drag, M.; Denault, J.-B. Molecular determinants involved in activation of caspase 7. *Biosci. Rep.* **2011**, *31*, 283−294.
(34) Martini, C.; Bedard, M.; Lavigne, P.; Denault, J.-B. Characterization of Hsp90 Co-Chaperone p23 Cleavage by Caspase-7 Uncovers a Peptidase-Substrate Interaction Involving Intrinsically Disordered Regions. *Biochemistry* **2017**, *56*, 5099−5111.
(35) Klaiman, G.; Champagne, N.; LeBlanc, A. C. Self-activation of Caspase-6 in vitro and in vivo: Caspase-6 activation does not induce cell death in HEK293T cells. *Biochim. Biophys. Acta, Mol. Cell Res.* **2009**, *1793*, 592−601.
(36) Srinivasula, S. M.; Ahmad, M.; Fernandes-Alnemri, T.; Alnemri, E. S. Autoactivation of procaspase-9 by Apaf-1-mediated oligomerization. *Mol. Cell* **1998**, *1*, 949−957.
(37) Renatus, M.; Stennicke, H. R.; Scott, F. L.; Liddington, R. C.; Salvesen, G. S. Dimer formation drives the activation of the cell death protease caspase 9. *Proc. Natl. Acad. Sci. U. S. A.* **2001**, *98*, 14250−14255.
(38) Inoue, S.; Browne, G.; Melino, G.; Cohen, G. M. Ordering of caspases in cells undergoing apoptosis by the intrinsic pathway. *Cell Death Differ.* **2009**, *16*, 1053−1061.
(39) Zou, H.; Henzel, W. J; Liu, X.; Lutschg, A.; Wang, X. Apaf-1, a human protein homologous to C.elegans CED-4, participates in Cytochrome c-Dependent Activation of Caspase-3. *Cell* **1997**, *90*, 405−413.
(40) Li, P.; Nijhawan, D.; Budihardjo, I.; Srinivasula, S. M; Ahmad, M.; Alnemri, E. S; Wang, X. Cytochrome c and dATP-dependent formation of Apaf-1/caspase-9 complex initiates an apoptotic protease cascade. *Cell* **1997**, *91*, 479−489.
(41) Han, Z.; Hendrickson, E. A.; Bremner, T. A.; Wyche, J. H. A sequential two-step mechanism for the production of the mature p17:p12 form of caspase-3 in vitro. *J. Biol. Chem.* **1997**, *272*, 13432−13436.
(42) Ponder, K. G.; Boise, L. H. The prodomain of caspase-3 regulates its own removal and caspase activation. *Cell Death Discovery* **2019**, *5*, 56.
(43) Lippke, J. A.; Gu, Y.; Sarnecki, C.; Caron, P. R.; Su, M. S.-S. Identification and characterization of CPP32/Mch2 homolog l, a novel cysteine protease similar to CPP32. *J. Biol. Chem.* **1996**, *271*, 1825−1828.
(44) Yang, X.; Stennicke, H. R.; Wang, B.; Green, D. R.; Janicke, R. U.; Srinivasan, A.; Seth, P.; Salvesen, G. S.; Froelich, C. J. Granzyme B mimics apical caspases: Description of a unified pathway for trans-activation of executioner caspase-3 and −7. *J. Biol. Chem.* **1998**, *273*, 34278−34283.
(45) Denault, J.-B.; Salvesen, G. S. Human Caspase-7 Activity and Regulation by Its N-terminal Peptide. *J. Biol. Chem.* **2003**, *278*, 34042−34050.
(46) Dagbay, K. B.; Hardy, J. A. Multiple proteolytic events in caspase-6 self-activation impact conformations of discrete structural regions. *Proc. Natl. Acad. Sci. U. S. A.* **2017**, *114*, E7977−E7986.
(47) Roschitzki-Voser, H.; Schroeder, T.; Lenherr, E. D.; Frolich, F.; Schweizer, A.; Donepudi, M.; Ganesan, R.; Mittl, P. R.E.; Baici, A.; Grutter, M. G. Human caspases in vitro: Expression, purification and kinetic characterization. *Protein Expression Purif.* **2012**, *84*, 236−246.
(48) Dagbay, K. B.; Hill, M. E.; Barrett, E.; Hardy, J. A. Tumor-Associated Mutations in Caspase-6 Negatively Impact Catalytic Efficiency. *Biochemistry* **2017**, *56*, 4568−4577.
(49) Tubeleviciute-Aydin, A.; Zhou, L.; Sharma, G.; Soni, I. V.; Savinov, S. N.; Hardy, J. A.; LeBlanc, A. C. Rare human Caspase-6-R65W and Caspase-6-G66R variants identify a novel regulatory region of Caspase-6 activity. *Sci. Rep.* **2018**, *8*, 4428.
(50) Slee, E. A.; Adrain, C.; Martin, S. J. Executioner caspase-3,-6, and-7 perform distinct, non-redundant roles during the demolition phase of apoptosis. *J. Biol. Chem.* **2001**, *276*, 7320.
(51) Alhadrami, H. A.; Hassan, A. M.; Chinnappan, R.; Al-Hadrami, H.; Abdulaal, W. H.; Azhar, E. I.; Zourob, M. Peptide substrate screening for the diagnosis of SARS-CoV-2 using fluorescence resonance energy transfer (FRET) assay. *Microchim. Acta* **2021**, *188*, 137.

https://doi.org/10.1021/acs.biochem.1c00459
Biochemistry 2021, 60, 2824−2835

(52) Julien, O.; Zhuang, M.; Wiita, A. P.; O'Donoghue, A. J.; Knudsen, G. M.; Craik, C. S.; Wells, J. A. Quantitative MS-based enzymology of caspases reveals distinct protein substrate specificities, hierarchies, and cellular roles. *Proc. Natl. Acad. Sci. U. S. A.* **2016**, *113*, E2001−E2010.
(53) Hill, M. E.; Kumar, A.; Wells, J. A.; Hobman, T. C.; Julien, O.; Hardy, J. A. The Unique Cofactor Region of Zika Virus NS2B-NS3 Protease Facilitates Cleavage of Key Host Proteins. *ACS Chem. Biol.* **2018**, *13*, 2398−2405.
(54) Zhou, J.; Li, S.; Leung, K. K.; O'Donovan, B.; Zou, J. Y.; DeRisi, J. L.; Wells, J. A. Deep profiling of protease substrate specificity enabled by dual random and scanned human proteome substrate phage libraries. *Proc. Natl. Acad. Sci. U. S. A.* **2020**, *117*, 25464−25475.

https://doi.org/10.1021/acs.biochem.1c00459
Biochemistry 2021, 60, 2824−2835